Ann. Geophys. Discuss., https://doi.org/10.5194/angeo-2019-26
Manuscript under review for journal Ann. Geophys.
Discussion started: 5 March 2019

Annales Geophysicae Discussions
Open Access

Evidence of vertical coupling: Meteorological storm Fabienne on 23 September 2018 and its related effects observed up to the ionosphere.

Petra Koucká Knížová[1], Kateřina Podolská[1], Kateřina Potužníková[2], Daniel Kouba[1], Zbyšek Mošna[1], Josef Boška[1] and Michal Kozubek[1]

[1]Department of Ionosphere and Aeronomy, Institute of Atmospheric Physics, Boční II/1401, 14100 Prague 4
[2] Department of Meteorology, Institute of Atmospheric Physics, Boční II/1401, 14100 Prague 4

Correspondence to: Petra Koucká Knížová (pkn@ufa.cas.cz)

Abstract: Severe meteorological storm system on the frontal border of cyclone Fabienne passing above Central Europe was observed on 23–24 September 2018. Large meteorological systems are considered to be important sources of the wave-like variability visible/detectable through the atmosphere and even up to ionosphere heights. Significant departures from regular courses of atmospheric and ionospheric parameters were detected in all analyzed data sets through atmospheric heights. Above Europe, stratospheric temperature and wind significantly changed in coincidence with fast frontal transition (100–110 km h^{-1}). Zonal wind at 1 and 0.1 hPa changes from usual westward before storm to eastward after storm. With this changes are connected changes in temperature where at 1 hPa analyzed area is colder and at 0.1 hPa warmer. Within ionospheric parameters, we have detected significant wave-like activity occurring shortly after the cold front crossed the observational point. During the storm event, both by Digisonde DPS-4D and Continuous Doppler Sounding equipment, we have observed strong horizontal plasma flow shears and time-limited increase plasma flow in both North and West components of ionospheric drift. Vertical component of plasma flow during the storm event is smaller with respect to corresponding values on preceding days.

Analyzed event of exceptionally fast cold front of the cyclone Fabienne fell into the recovery phase of minor-moderate geomagnetic storm observed as a negative ionospheric storm in European Mid-latitudes. Hence, ionospheric observations consist of both disturbances induced by moderate geomagnetic storm and effects originated in convective activity in troposphere. Nevertheless, taking into account significant change in global circulation pattern in the stratosphere, we conclude that most of the observed wave-like oscillations in the ionosphere during night 23–24 September can be straight attributed to the propagation of atmospheric waves launched on the frontal border (cold front) of the cyclone Fabienne. Frontal system acted as an effective source of atmospheric waves propagating upward up to the ionosphere.

Ann. Geophys. Discuss., https://doi.org/10.5194/angeo-2019-26
Manuscript under review for journal Ann. Geophys.
Discussion started: 5 March 2019

1 Introduction - Variability of the ionosphere

Ionosphere is highly variable system that is influenced by solar and geomagnetic activity from above and lower-laying atmospheric phenomena from below. Ionospheric variability is observed on a wide-scale range from minutes, or even shorter, up to scales of solar cycle and secular variations of solar energy input. With no doubt, the most dominant driver of ionospheric variability is solar activity. Whole atmosphere and ionosphere react according to the level of solar energy input. The episodes of limited strongly enhanced dissipation of solar energy (solar flares, coronal mass ejections etc.) can affect only regions localized in high latitudes or can cover all the geosphere. During such event, the magnetosphere is affected first (see for instance Hargreaves,1992). A large portion of solar energy is dissipated in the upper atmosphere and then in the ionosphere, thermosphere (Davies, 1990; Solomon and Qian, 2005). The perturbations can be detected at the ground level, for instance by magnetometers. Disturbances associated with such enhanced solar energy inputs are in general called geomagnetic storm (Gonzales et al., 1994, Buonsanto, 1999) or geospheric storms (Prölss, 2004). Different types of solar agents that are mainly responsible for geomagnetic disturbances have been analyzed with respect to their geoeffectiveness by Kakad et al. (2019), Georgieva et al. (2006), Fenrich and Luhmann (1998), Leamon et al., (2002), Prölss (2004) and many others.

Besides the solar and geomagnetic forcing the energy inputs from lower-laying atmospheric heights must be taken into account in the energy budget of the ionosphere. The lower laying atmosphere and its impact on the ionosphere have been largely studied during last exceptionally low solar cycle by mean of growing number of satellite measurements. Paper Anthes (2011) and more recent paper Liu at al. (2017) demonstrated effectivity of Radio Occultation (RO) sounding methods on board of satellites for systematic sounding of the atmosphere with respect to weather, climate and space weather.

Ionosphere is weakly ionized plasma where both neutrals and ions play an important role. Ionization degree around maximum of electron concentration is less than 10^{-2} and significantly smaller below the maximum in the F layer, except limited events of Sporadic E layer occurrence (Whitehead, 1961,1990; Mathews, 1998; Haldoupis, 2012). The impact of the collision processes on the ionospheric dynamics cannot be neglected especially in the lower ionosphere. During day time, due to incoming solar radiation, ionosphere is formed at height of mesosphere and thermosphere. Ionosphere is typically stratified into D, E and F layer, where the maximum electron concentration is usually located. The F layer is usually a region with maximum electron concentration. It can be split into two sub layers denoted F1 and F2 layers. In case of splitting into F1 and F2 layers, the maximum of electron concentration is located in F2 layer. During night time electron concentration decreases at all heights due to recombination processes and lack of ionizing radiation. It leads to practical disappearance of all ion pairs below F layer that remains present due to slow recombination processes at its height (Davies, 1990; Rishbeth, 1998; Prölss, 2004 among many others). As a measure of the ability of the Earth´s atmosphere to absorb incoming solar radiation we can consider the maximum electron concentration NmF2 in the highest ionospheric level F or F2 if present. During solar cycle, we can observe clear link between incoming solar radiation and

Ann. Geophys. Discuss., https://doi.org/10.5194/angeo-2019-26
Manuscript under review for journal Ann. Geophys.
Discussion started: 5 March 2019

ionospheric ionization. With the increasing solar activity we observe higher ionization. However, the relationship is not linear and is subject of large investigation. The link between ionospheric variability and both solar and geomagnetic indices were analyzed for instance by Clilverd et al., 2003; Cnossen et al., 2014; Forbes et al., 2000; Roux et al., 2012; Koucká Knížová et al., 2018, Perrone et al., 2017. Understanding of the relation between solar activity and corresponding ionospheric and/or atmospheric behavior is crucial for instance in the estimation of the trends and potential human impact on the atmosphere and ionosphere (Roininen et al., 2015; Laštovička et al., 2012; Laštovička, 2012; Georgieva et al., 2012).

Ionosphere clearly reflects solar activity on all studied time-scales. Diurnal courses of the maximum concentration in the ionosphere clearly show the dominant solar influence, increase/decrease of the electron concentration with respect to solar zenith angle. During stable solar and geomagnetic situation, however, significant difference in the courses of ionospheric parameters is well seen on consequent days. Vertically propagating gravity waves are subject of large scientific interest since 1960s. A fundamental interpretation of atmospheric variability in terms of atmospheric gravity waves was provided by Hines (1960) and later by Hines (1963, 1965, 1968 among others). The effects of gravity waves on in the ionosphere up to F2 region through photochemical and dynamical processes were discussed by Hooke (1970b). Garcia and Solomon (1985) reported GW importance on the chemical composition of the middle atmosphere. There, it has been already shown that the resulting effects of gravity waves depend not only on the wave properties but on the actual ionospheric situation and/or direction of propagation with respect to incoming solar radiation (Hooke, 1970a; 1971). It has been pointed out by Holton (1983) that gravity wave drag and diffusion are fundamental for the wind and temperature balance in the middle atmosphere. Fritts and Nastrom (1992) suggested that convective activity in the troposphere is as important source of gravity waves as topographic forcing. Model study of gravity wave generation and its observable signatures above deep convection is provided by Alexander et al. (1994). Later detail model studies of gravity wave propagation through the Earth's atmosphere simulations provided by Vadas and Fritts (2005), Vadas (2007), Vadas and Nicolls (2012) proved that gravity waves originating in the tropospheric convection can reach thermospheric heights and significantly affect wind and temperature profiles. Atmospheric waves propagate from lower laying atmosphere up to the thermosphere as primary waves or dissipate. The deposited momentum excites secondary waves (see for instance Vadas and Liu (2009) or Vadas et al. (2018)).

Except model studies there are observational evidences of consequent ionospheric disturbances attributed to dynamical processes in the lower atmosphere. Chernigovskaya et al. (2018) provides an evidence of F2-layer ionospheric response to dynamic processes during the winter circumpolar vortex evolution in the strato-mesosphere. McDonald et al., (2018) reported an enhancement in total electron content in ionosphere, which coincides with the commencement of a stratospheric warming event. Goncharenko et al. (2010) observed persistent variations in the low-latitude ionosphere that occur several days after a sudden warming event in the high-latitude winter stratosphere. Enhancements of wave-like activity within ionospheric F layer with relation to meteorological events were reported by Chernigovskaya et al. (2015). Propagation of concentric gravity waves from source region in the troposphere related to tropospheric convective storm up to the ionosphere was reported by Azeem et al. (2015). Paper presents almost simultaneous observations of a gravity wave event in the stratosphere, mesosphere, and ionosphere. Suddenly increasing wave-like oscillations within ionospheric parameters after passing tropospheric cold front across observational point

Ann. Geophys. Discuss., https://doi.org/10.5194/angeo-2019-26
Manuscript under review for journal Ann. Geophys.
Discussion started: 5 March 2019

was reported by Boška and Šauli (2001) and Šauli and Boška (2001). On the longer term-term scale, the extremely high correlation between ionospheric measurements of the up to the 'break point' at 10 degrees in longitude and/or Earth´s distance 1000 km is attributed to the mesoscale systems as proposed by Koucká Knížová et al. (2015). Infrasound waves excited by severe tropospheric storms (e.g. typhoons and strong storms) are discussed and analyzed. Chum et al. (2018) detected infrasound in the ionosphere from earthquakes and typhoons, by mean of Multipoint Continuous Doppler Sounding equipment. Authors give examples of observation by an international network of continuous Doppler sounders. The waves were observed at the height range from about 200 to 300 km by continuous Doppler sounder located in Taiwan (Chum et al., 2018). The infrasound was observed during several hours for strong storms events.

Review of lower atmosphere forcing was provided by Lastovička (2006). Review of coupling processes in the atmosphere with respect to atmospheric waves and sudden stratospheric warmings can be found in Yigit et al. (2016). The importance of involvement of lower atmosphere into ionospheric variability study in order to accurately capture smaller-scale features of the upper atmosphere response even to the geomagnetic storms, is demonstrated by Pedatella and Liu (2018). The evidence of lower atmosphere forcing is clearly demonstrated on the day-to-day ionospheric variability (known as an ionospheric anomaly) during low and stable solar and geomagnetic activity during consequent days. Ionospheric parameters (e.g. electron concentration or height of ionospheric layers) on such scales are influenced by combination of meteorologic activity and solar/geomagnetic forcing. During geomagnetically quiet days the tropospheric forcing is more emphasized and relatively more important and is ruling the ionospheric dynamics, far more than the solar and geomagnetic energy inputs.

2 Data

For the description of cyclone Fabienne in the troposphere we use **meteorological** ground-based data (https://www.ventusky.com/, www.wetterkontor.de, http://wetter3.de, http://www.ufa.cas.cz/institute-structure/department-of-meteorology/present-weather-sporilov.html) and Aeolus satellite measurements described in the following chapter 2.1. Behavior of the stratosphere is interpreted using **stratospheric** wind and temperature reanalysis MERRA 2 datasets (https://disc.gsfc.nasa.gov/daac-bin/FTPSubset2.pl) described in chapter 2.2. The ionosphere observation (details are provided in chapter 2.3) comes from two ground based vertical **ionospheric** sounding using the Digisonde DPS 4D (http://giro.uml.edu/ and http://digisonda.ufa.cas.cz/) and oblique reflection using the multipoint Continuous Doppler Sounding (CDS) http://www.ufa.cas.cz/files/OHA/M_Doppler_system.pdf. Besides that we use satellite TEC measurement (http://gnss.be/Atmospheric_Maps/ionospheric_maps.php) for station Pruhonice. For geomagnetic situation description we use geomagnetic indices from Potsdam Data Center https://www.gfz-potsdam.de/en/kp-index/. The data used for interpretation of Fabienne event and related disturbances in stratospheric and ionospheric heights cover time interval 20–27 September 2018.

Ann. Geophys. Discuss., https://doi.org/10.5194/angeo-2019-26
Manuscript under review for journal Ann. Geophys.
Discussion started: 5 March 2019

2.1 Meteo data

In order to describe severe storm Fabienne we use ground-based meteorological monitoring combined with satellite observation. For determination of the synoptic condition in the troposphere, surface and upper synoptic maps were used (available at https://www.wetterkontor.de/ and http://wetter3.de). We also used **meteorological** ground-based radar observations taken from the https://www.ventusky.com/. In addition hourly averages meteorological data performed by automatic weather station located at the Institute of Atmospheric Physics IAP (50.04°N, 14.48°E) were used for determining the time of frontal passage (http://www.ufa.cas.cz/institute-structure/department-of-meteorology/present-weather-sporilov.html). Data are available for last 30 days, then they are stored in the institute archive.

The Earth Explorer Atmospheric Dynamics Mission Aeolus yields data from global observations of wind profiles from space using the active Doppler Wind Lidar (DWL) method (Gompf, 2000). The DWL measurement is the unique method that has the potential to provide the required data on a global scale, from direct observation of wind. The DWL measures 100 wind profiles per hour using both Rayleigh and Mie scattering method (Durand et al., 2004). The global wind profiles (along a single line-of-sight) are measured up to an altitude of 30 km to an accuracy of 1 m s^{-1} in the planetary boundary layer (up to an altitude of 2 km). The Aeolus mission was launched on 22 August 2018 and scientific measurement started on 12 September 2018.

2.2 Stratospheric Data

The MERRA2 (Modern-Era Retrospective analysis for Research and Applications, version 2 from https://disc.gsfc.nasa.gov/daac-bin/FTPSubset2.pl) with resolution 0.5° in latitude and 2/3° in longitude was used. The MERRA-2 is a global atmospheric reanalysis produced by the NASA Global Modelling and Assimilation Office (GMAO), details can be found in Gelaro et al. (2017). The MERRA2 is available up to 0.1 hPa from 1980 till presents but we show only 1 and 0.1 hPa for period from 20 September 2018 to 27 September 2018 which is relevant for our studies. This reanalysis provides reliable time series in regular gridded network. Temperature and zonal wind 6-hourly data (00, 06, 12 and 18 UT) in the stratosphere and lower mesosphere (from 30–80 km) was used. The MERRA 2 reanalysis has many advantages as reliable time series without gaps, regular gridded network or high vertical resolution. Of course there are some disadvantages. Because reanalysis include many observations datasets from satellite, radiosondes or ground measurements they have to be assimilated into one dataset. That is why we can get biased dataset especially at higher altitudes. On the other hand, we need only qualitative description of the stratosphere for our study.

2.3 Ionospheric Data

State of the ionosphere is monitored on a regular base beginning setting of the network of ionosondes in frame of the International Geophysical Year in 1957–1958. Some of the

Ann. Geophys. Discuss., https://doi.org/10.5194/angeo-2019-26
Manuscript under review for journal Ann. Geophys.
Discussion started: 5 March 2019

ionospheric station are still operating and represent observatories with longest time series of ionospheric data available for research.

Vertical sounding of ionosphere is based on the reflection of electromagnetic wave from ionospheric plasma. Sounding pulse is reflected from plasma unit when the sounding frequency is equal to its plasma frequency (see for instance Davies (1990)). Using typical sounding frequency range 1 MHz–20 MHz it is possible to monitor ionosphere from the E layer up to maximum electron concentration in the F region. With increasing frequency of the sounding wave, the pulse penetrates higher to the ionosphere. When the frequency of the sounding pulse exceeds plasma frequency of maximum, the pulse propagates through the ionosphere without reflection and no echo is registered in the receiver. Maximum frequency of the reflected wave from the particular layer is called critical frequency and is simply related to maximum plasma concentration of the layer. For the purpose of the analyses we use maximum of electron concentration NmF2 located in the F or F2 layer, and the corresponding plasma frequency called critical frequency and denoted foF2. Time series of foF2 are the longest data sets available for systematic study of ionospheric variability.

In the Observatory Pruhonice (49.9°N, 14.6°E) located close to Prague, Digisonde DPS 4D is used for regular ionospheric monitoring. Digisonde DPS 4D provides ionograms, directograms and skymaps for further evaluations and interpretations. Digisonde operates in the multi-beam sounding mode using six digitally synthesized off-vertical reception beams in addition to the vertical beam. For each frequency and height on a multi-beam ionogram, the raw data from the four receive antennas are collected and processed to form seven beams, separately for the O-mode and X-mode echoes (Reinisch, 1996; Reinisch et al., 2005). Detail description can be found also on web page http://umlcar.uml.edu/digisonde.html.

All the data were manually checked and evaluated. Detail processing of the drift measurement and how the skymaps are controlled, is described by Kouba at al. (2008) and Kouba and Koucká Knížová (2012). High-rate sounding campaign partly overlap our selected time span. The aim of the high-rate sounding measurement was to monitor short-term variability of the Es-layer. Hence, our data consists of data with 2-minutes (till 24 September at 6:30 UT) and 15-minutes repetition time. Ionospheric drift data are not yet widely used for description of ionospheric variability. Kouba and Koucká Knížová (2016) have provided first systematic study of regular course of vertical drift component in Mid-latitudes. The study was conducted during year 2006, i.e. during time interval described by low solar and geomagnetic activity. It shows diurnal and seasonal variability of the vertical plasma drift component and quantifies its characteristic values.

Ionogram represents height-frequency characteristics of the ionosphere above the station. It displays virtual reflection height vs. sounding frequency. Using only vertical echo on the ionogram one can receive height profile of frequency or electron density (Davies, 1990 and many others). According to the receiving antenna field, multi-beam ionograms can be recorded. Digisonde can register off-vertical reflections in addition to the vertical one. The off-vertical signals are further processed to show characteristics of the oblique reflection caused by ionospheric irregularities. Directogram (see for more detail description http://ulcar.uml.edu/directograms.html) provides information about direction of the echoes received from irregularity. The central column between the panels corresponds to the vertical reflection at zero zenith angle. Shades of blue in the directogram correspond to general direction of plasma-drift from west to east, and shades of red are used to represent drift in the opposite direction, i.e. from east to west.

In addition to Digisonde DPS-4D, ionosphere is regularly monitored by a multi-point continuous Doppler (CDS) sounding portable system based on the measurements of the Doppler shift experienced by waves reflected from the ionosphere. The measurements are simultaneously performed on 3 to 5 frequencies with 4 Hz separation around the center frequency of 3594.5 kHz. Multipoint measurement makes it possible to investigate propagation of infrasonic waves or ionospheric oscillations caused by fluctuations of geomagnetic field etc. (http://www.ufa.cas.cz/files/OHA/M_Doppler_system.pdf). Observation of wave propagation in the ionosphere was performed on the basis of multi-point and multi-frequency continuous Doppler sounding (CDS) in the Czech Republic. We used two multi-point CDS systems operating at frequencies of 3.59 and 4.65 MHz. Kouba and Chum (2018), demonstrated efficiency of Digisonde-based drift measurement together with Continuous Doppler Sounding on fixed frequency for study of dynamics of the ionosphere. Chum et al. (2018) detected infrasound waves generated by seven typhoons that passed over Taiwan or in its surroundings in period 2014–2016. The spectral characteristics of the ionospheric infrasound from convective storms are sensibly similar as for the cotyphoon infrasound. The highest spectral densities were observed during about 2–5 minutes (3.3–8.3 mHz).

The ground-based ionospheric sounding was complemented by Total Electron Content (TEC) above station Pruhonice derived from satellite measurement (http://gnss.be/Atmospheric_Maps/ionospheric_maps.php). While the foF2 parameter describes local maxima of electron concentration, and thus the variation of foF2 can be attributed mostly to the ionization-recombination processes in the F2 region the TEC satellites measurement is a parameter representing integral of electron concentration from bottom to upper part of the ionosphere.

3 Meteorological description of storm Fabienne

Synoptic evolution: On 20 September 2018 a short-wave travelled eastward from the British Isles towards Sweden and Poland and supports strengthening of a cyclone Elena over the North Sea. Anticyclonal warm late summer condition with weak southwest flow occurred in Central Europe. A strong frontal zone from the north Atlantic over the Central Europe separated cool Atlantic air from the hot continent. The unusually hot and dry weather in the Central Europe culminated September 21 afternoon and accelerate the movement of cold front around noon. Along the front there was forming squall line with thunderstorms in the evening. Recorded strong wind gusts were caused by both convective activity and a significant pressure gradient within the cyclone.

During the following days, the low descent centre moved towards the northeast and formed a deep cyclone above Scandinavia. Because of the strong zonal flow along the lower edge of this cyclone another front system coupled with the Fabienne cyclone quickly moved to Central Europe. On 23 September the cyclone Fabienne deepened and passed through Central Europe to the east. Within the warm sector ahead of a cold front of the Fabienne humid low-level air is advected northeastward from the subtropical North Atlantic. This resulted in evolving intense convection and formation squall line with thunderstorms along the very fast moving cold front. Synoptic time-evolution is demonstrated in the Figure 1.

Surface data: In Figure 2. There are average hourly data measured at Institute of Atmospheric Physics (IAP) meteorological station clearly show the cold front that passed over this station at 18 UT on 21 September, when ground level pressure reached a local minimum. Before the front, maximum air temperatures at 2m reached tropical values above 30 °C, behind the front the maximum daily temperature did not reach more than 20 °C. The average hour wind speed intensified before the front and during the rainfall associated with storm activity. After passing the front, the surface wind changed from southwest to northeast.

Around 15 UT the warm front brought light rain associated with stratiform clouds. The temperature at 12 UT on September 23 was lower than in the afternoon when the area was temporarily in the warm sector of cyclone Fabienne. Lifetime of the warm sector was very short. The time-series of surface variables at IAP station show the warm front which is connected with slight direction windshift, but rapid rise in temperature until 18 UT on September 23. At this time the passage of the cold front connected with Fabienne occurred and brought a thunderstorm activity with heavy rain and wind shock. The surface pressure minimum was close to 1000 hPa, while the temperature reached local maximum and the wind direction changed from from west to north. The hourly mean wind speed rose rapidly up to midnight. On September 24 was cold, the maximum temperature reached only 12.8 °C. The strong cold northwest wind remained across the measurement point, the maximum averaged hourly values reached 7 m.s^{-1} in the afternoon. Pressure continued to rise until midnight following day. Centre of the massive anticyclone Shorse (see Figure 1), which moved from the British Island over the Czech Republic in just 36 hours brought the pressure to a value of 1040 hPa.

Both the Europe surface pressure charts in Figure 1 and the ground level time series for IAP observatory in Figure 2 displays unusually fast passage of synoptic pressure patterns over the Central Europe. Cyclone Fabienne moved at around 25 m.s$^{−1}$. It exceeds speeds of extratropical transition. Jones et al. (2003) described extratropical transition of tropical cyclones which can accelerate from a forward speed of 5 m.s$^{−1}$ in the Tropics to more than 20 m.s$^{−1}$ in the Mid-latitudes. Sanders (1986) noted mean surface cyclone speed of moving of about 18 m.s$^{−1}$ for cyclone originated in the west-central North Atlantic and deepened explosively. A manual in Czech language based on both empirical observations and classical synoptic meteorology states that the average cyclones speed over Europe is around 8 m.s$^{−1}$ to 11 m.s$^{−1}$ (Kopáček, Bednář, 2009)

The synoptic-scale windstorm connected with the cyclone Fabienne is an unusual event for the time of occurrence (23 September 2018) and for the storm moving velocity and intensity (Kašpar et al, 2017). The month of September in the Middle Europe is typically characterized by significant condition under high pressure, i.e. relatively weak wind sunny days. Figure 3 exhibited the fast moving of cyclone Fabienne in a strong zonal flow from Atlantic region across the Central Europe. Within the warm sector of the cyclone unstable wet air has been advected from subtropical Atlantic region to northest-ward perpendicular to the direction of cyclone moving. Follow-up strengthened baroclinity of the atmosphere at lower levels was the main cause of quick cyclone deepening (visible on surface pressure field - white lines) and generated storms at the head of the cold front.

The 500 hPa map shows the main flow regime of the troposphere. (The atmosphere at an altitude about 5.5 km is no longer under the influence of surface friction. In synoptic meteorology 500 hPa map is used to determine the speed and direction of synoptic patterns.) In the morning on 23 September the density of isohyps depicted at 4-decameters interval indicated a large pressure gradient between the warm southern and cold northern parts of Europe. At 12 UT the cyclone center is still located above Germany at 18 UT it is above the territory of the Czech Republic. On the 850 hPa pseudopotential maps there are clearly visible narrow transformation zones with a strong gradient of pseudopotential temperature. These "warm boundaries" are separated various homogenous air masses with different temperatures and locate the position of the fronts on the surface pressure field Kašpar (2003) (http://www.met.wur.nl/education/atmospract/unit9/thetaw%20and%20fronts.pdf). From radar images presented on Figure 4, the speed of the squall line can be estimated at 110 km/h. Impacts of the strong wind gusts associated with this squall line passage have been well documented on the European Severe Weather Database (https://www.eswd.eu).

Satellite Aeolus observation provides global wind profiles (along a single line-of-sight) up to an altitude of 30 km with an accuracy of 1 m s^{-1} in the planetary boundary layer (up to an altitude of 2 km). The Aeolus mission was launched on 22 August 2018 and scientific measurement started on 12 September 2018. The Earth Explorer Atmospheric Dynamics Mission Aeolus yields data from global observations of wind profiles from space using the active Doppler Wind Lidar (DWL) method (ESA, 1989; Durand et al., 2004). The DWL measurement is the unique method that provide data on a global scale from direct observation of wind. The Aeolus Doppler Wind Lidar measures 100 wind profiles per hour using both Rayleigh and Mie scattering method (for more information see https://earth.esa.int/web/guest/missions/esa-operational-eo-missions/aeolus).

The graphs in Figure 5 display the wind profiles measured by Aeolus ESA satellite using ALADIN instrument during the time period from 22–24 September 2018 (orbit numbers 481 to 520), geographical coordinates ranges: 12°–19° E, 48°–51° N; geomagnetic coordinates: 97° L, 48° F, -17° Y. The vertical axes represent altitude of height bins, while the horizontal axes represent time of observation. Data catalogue is provided by ESA EO, from http://aeolus-ds.eo.esa.int/socat/L1B_L2_Products.

4 Stratospheric dynamics 20–27 September 2018

Stratosphere and its dynamics is very sensitive for wave activity in higher or lower layers (troposphere or mesosphere). That is why a strong storm Fabienne as a source of many different kind of waves should bring disturbance into regular dynamics. With changes in dynamics are connected changes in temperature and vice versa. Stratospheric wind and temperature for Europe region are presented for time span 20 September at 00 UT to

Ann. Geophys. Discuss., https://doi.org/10.5194/angeo-2019-26
Manuscript under review for journal Ann. Geophys.
Discussion started: 5 March 2019

September 27 at 18 UT. This period covers whole week (3 day before and 4 after Fabienne storm).

Figure 6a shows zonal wind at 1 hPa for Europe region from 20 September at 00 UT to 27 September at 18 UT. On the sequence there is well seen weak eastward wind in middle Europe and westward wind in south Europe which is typical situation for this period. Shortly before storm Fabienne easterly wind became stronger (because of incoming waves from troposphere) and remain easterly for the following several days. At 1 hPa stratosphere needs some time for changing/restoration dynamics to normal situation because of wave disturbances which remains in inversion condition (temperature increase with altitude) much longer than in other layers. That is why we can observe strong eastward wind not only during the storm but for several days after storm in whole Europe as well.

The changes in the zonal wind, which mainly control stratospheric dynamics (meridional wind is much weaker but very important for Dobson-Brewer circulation), are usually connected with changes in temperature because strong zonal wind effectively block air mixing form different latitudes especially in higher latitudes. The temperature is observed directly so we can expect better approximation in reanalysis than for zonal wind which is derived parameter. The temperature fields at 1 hPa are presented on Figure 7a. We can find much colder air in middle and northern Europe after storm Fabienne because usual strong barrier between high and lower latitudes are destroyed after Fabienne and much colder air from polar vortex can reach lower latitudes in our case middle and south Europe. Colder air in lower latitudes for several days after storm Fabienne could impact not only chemistry in higher stratosphere in autumn but mesosphere condition as well (i.e. the propagation of waves could be slower or faster than usual or they can be absorbed in the stratosphere)

At 0.1 hPa (on the Figure 6b) the change of the zonal wind is even stronger than at 1 hPa (compare Figure 6a and b) because the wind in the mesosphere is usually stronger than in the stratosphere. Several hours after storm zonal wind changes from westward or very weak eastward to strong eastward and remains without changes for several days. Meridional wind in mesosphere is stronger than in the stratosphere but still zonal wind plays major role in the dynamics changes. Temperature changes at level 0.1 hPa, that corresponds to lower mesosphere, are opposite from pressure level 1 hPa. There is warmer air in higher latitudes so stronger eastward wind brings this warmer air to the lower latitudes (because it is not blocked by the westward wind) and affects the whole area of the middle Europe. The warmer air stays in analyzed area because the zonal wind has to reverse to his usual state (westward instead of eastward). We have to notice that 0.1 hPa is above stratosphere and the dynamics here could be affected by different processes (i.e. solar radiation, chemistry etc.) than at 1 hPa (almost stratopause).

Especially 0.1 hPa are on the top of the MERRA2 reanalysis so we should be very careful with interpretation of the results because the information from this level could be affected by border condition or problem with wave activity dissipation. But we need mainly qualitative description rather than quantitative description for our study so information from MERRA2 are sufficient.

5 Geomagnetic Situation – Preceding moderate storm

September 2018 was a period of rather low geomagnetic activity. On 4 September the geomagnetic activity increased for about 20 hours. Maximum registered Kp index was Kp = 6. The following period was characterized by low geomagnetic activity with Kp up to 3 till September 18 when the Kp index fall down to 0 and remain very low till September 21. On September 21 the geomagnetic activity increased again at 22:30 UT when Kp = 4+. Increased geomagnetic activity lasted for about 20 hours with maximum Kp = 5- on 23 September at 03 UT. The activity can be classified as a minor to moderate geomagnetic storm. On 23 September, the geomagnetic activity fall again to values around Kp = 2 to 2+. In general, there was rather low geomagnetic activity with only short slightly enhanced events. However, the geomagnetic effects are responsible for part of the observed ionospheric variability and cannot be completely neglected. Geomagnetic indices were downloaded from Potsdam Data Center https://www.gfz-potsdam.de/en/kp-index/.

6 Ionospheric dynamics and wave activity

An example of multi-beam ionograms measured by DPS-4D is shown on the Figure 8. There is a sequence of ionograms recorded during four consequent days around 23 UT. Colors of echo indicate particular direction of arrival. It is clearly shown that echo changes significantly. Ionogram at 23 UT is selected to show changing dynamics of the ionospheric plasma. During night time, ionograms with clear echo are typically recorded. Antenna system registers practically only vertically reflected signal, as it is shown on panel (a) measured on 22 September and panel (d) recorded on 25 September. In comparison, qualitatively different pattern is detected on panels (b) and (c). The echo on panel (b), recorded on 23 September shortly after passage of the cold front with heavy storm activity, is called spread F situation. As it is indicated by color scheme on the right side of each ionogram, antenna system records echo from practically all sounding beams. Both vertical and off-vertical echoes are spread in height and frequency. It means that ionosphere is full of irregularities and iso-contours of electron concentration are significantly undulated. On the panel (c) measured on 24 September, there is well recorded vertical echo and slightly higher oblique structure reflected from North-North-East direction. Such kind of echo is known as spur echo and may appear when ionospheric iso-contours are significantly tilted. In general, vertical echo on panel (c) correspond to situation on panels (a) and (d). Spread F situation on panel (b) indicates significant wave-like activity within ionospheric plasma in the F-region.

Sequence of directograms recorded by DPS-4D is shown in Figure 9. There are two episodes of increased activity clearly highlighted. On the directograms measured first two days 21–22 September, wave activity is rather low. Situation changes significantly on 23 September at 17 UT when strong echo is recorded till 24 September at 4 UT. Signal detected by the receiver varies significantly during night. An interesting fact is that DPS-4D instrument detects strong quickly changing plasma shears and reversal plasma motion with respect to zero zenith-angle. There is no prevailing or characteristic plasma flow for the event. During day-time, there is very low activity visible on the directogram till evening hours. Strong echo

Ann. Geophys. Discuss., https://doi.org/10.5194/angeo-2019-26
Manuscript under review for journal Ann. Geophys.
Discussion started: 5 March 2019

is recorded again from 24 September at 17 UT till 25 September at 4 UT. However, the echo is not as strong as the preceding night with smaller shears. Prevailing or dominant plasma motion during local night 24–25 September is in North-North-East direction.

On the plot of the diurnal course TEC in Figure 10 (a), decrease can be observed on 23–24 September compared to previous day September 22nd. Similarly in Figure 10 (b), decrease in critical frequency foF2 was observed during 23–24 September. Both values agree well through the studied interval and their matching can be explained by dominant contribution of F2 layer's electron contribution to the TEC and much less contribution of E layer's variability during studied days, even during the Fabienne event. The effect of electron concentration decrease in the ionosphere can be attributed to the geomagnetic disturbance observed as a negative storm effect (Prölss, 2004) related to the decrease of the atomic oxygen leading to decrease of production of oxygen ions and the increase of molecular nitrogen density leading to the increase of loss rate of ion species. Both processes lead to electron-ion concentration decrease. Values of critical frequencies foF2 and TEC return to typical values of the season comparable with those preceding the observed geomagnetic storm event on 25 September (two day after the storm passage over Pruhonice station). Geomagnetic disturbance started on 21 September at 21 UT. Frequency foF2 during night falls much faster than it is typical. Then foF2 oscillates and remain below 3.5 MHZ till almost noon when rapidly increases. During night 23–24 September, after sunset critical frequency foF2 decreases faster compare to nights 21–22 September and 25–26 September, when typical course of foF2 is registered.

All ionograms were manually scaled and further used for determination of vertical profile of electron concentration (or frequency) with the use of NHPC inversion technique that is part of the digisonde software. Details and downloads are available on web page: http://umlcar.uml.edu/digisonde.html. In agreement with course of foF2 and TEC, analyses of entire electron density profiles reveal same decrease on 23–24 September as a consequence of the preceding geomagnetic moderate storm. In order to illustrate well the electron concentration variability related to cold front effect we focus on profilograms for three consequent days 22–23 September.

Further we focus on three days of 22–24 September. Due to geomagnetic disturbance electron concentration and corresponding plasma frequency decrease which leads to problematic representation of the situation for entire time-span 21–26 September. Figure 11 shows variations of reflection height of the sounding signal recorded on 22–24 September for selected range 2–6 MHz with 0.1 MHz step. Oscillations in heights clearly show strong wave-like activity within all ionospheric heights. Comparing reflection heights at fixed frequencies for two consequent nights, there are shorter period oscillations visible during night on 22–23 September compared to night-time on 23–24 September. Oscillations detected during both nights are coherent through all levels.

Similar effects of oscillation (on Figure 11) are seen on the detail plot of profilograms Figure 12 composed from true-height profiles during all analyzed days. Deviation from regular course is well seen on profile thickness that is significantly smaller on 23 September till 24 September about 6 UT, when thickness of profiles increases again.

Further we have analyzed critical frequency foF2 using continuous wavelet transform to obtain power content on particular periods. Wavelet Power Spectra (WPS) for 21–26 September is presented on the Figure 13. Oscillations on shorter periods on 22 September compared to 23 September are well seen in Figure 13. In the plot of WPS, there are high power domains of short-period oscillation in the range 5–30 minutes during day-time on 21 September and 22 September. Less energy is detected during day-time on 23 September. Missing spectral content on periods below 30 minutes on 24–26 September is caused by change of sounding rate on 24 September at 10 UT. As it has been explained in data section, high sampling rate campaign was switched till morning on 24 September for study of Sporadic-E phenomenon.

Following three panels in Figure 14 show the ionospheric drift evolution 20 September–27 September. In the plots of North (panel b) and East (panel c) components, during several days preceding both geomagnetic and meteorological storm there are only rare situations where the ionospheric plasma motion was detected in a horizontal plane. Episode of longer duration of plasma flow in the horizontal plane is detected after sunset on 23 September when the storm Fabienne hit observation point. Characteristic value of plasma flow velocity is $\boldsymbol{v}_{North}$ ~ 40 m.s^{-1} and $\boldsymbol{v}_{East}$ ~ - 30 m.s^{-1}. Comparing North component of the plasma flow during night of the Fabienne storm (24 September, at 1 UT–4 UT) and corresponding time following days, it is important to point out that the flow is in opposite direction and practically same velocity magnitude.

Vertical components in Figure 14 (a) show typical diurnal course with two minima, one located close to sunrise and one close to sunset (same as reported by Kouba and Koucká Knížová, 2016). Values of vertical drift before Fabienne storm event reached regularly larger values with respect to days after the event. For instance, magnitudes of sunrise negative velocity peaks are detected around ~ - 50– - 30 m.s^{-1} , while after the event sunrise peaks are not exceeding ~ - 20 m.s^{-1} . The abrupt change is seen on 23 September at 19 UT, soon after the cold front passing above the observation point. Characteristic values before storm are exceeding $\boldsymbol{v}_v$ ~ 20 m.s^{-1}, while after the storm they hardly reach $\boldsymbol{v}_v$ ~ 20 m.s^{-1} and rather stay close $\boldsymbol{v}_v$ ~ 10 m.s^{-1}. Change in plasma flow is well pronounced in all three drift velocity components shortly after the frontal passage above observational point at ground level.

In the following Figure 15, we show Continuous Doppler Sounding (CDS) measurement on three consequent days 22–24 September on frequency 3.59 MHz (a) and 4.65 MHz (b). Beginning the storm Fabienne (or passage above observational point) is visible in the data as a short-duration increase of noise across the CDS spectra on both frequencies, Qualitative change of the echo is evident for the first sight. Data were obtained from Continuous Doppler Sounding spectrogram archive IAP CAS, Prague, http://datacenter.ufa.cas.cz/. Spectrograms of the recorded infrasound during event Fabienne until 4 UT correspond to the reference time for this event**.** The spectral content changed with time and was different during the strong storm event compare to preceding and following day.

Period of perturbations was observed until around 4 UT. The occurrence of stronger echo on CDS sounding on 3.59 MHz corresponds to the increased wave activity on directograms and detection of plasma flow on both North and East plasma drift components. According to our experience in Chum et al. (2018) we can conclude that we observe disturbances related to waves propagating from lower-laying atmosphere. It was shown that the cotyphoon infrasound waves were recorded in the spectral range from ~3.5 to 20 mHz with maximum of spectral density around 5 mHz (dominant periods between 3 and 4 minutes). The spectra revealed fine structures that were likely caused by modal resonances.

7 Conclusion

We have analyzed atmospheric and ionospheric effects induced by fast transit of cold front with strong storm of the cyclone Fabienne. Cold front passed above Europe within 24 hours with high speed reaching values 30 m.s^{-1} (approx. 108 km.h^{-1}) on 23 September 2018. The synoptic-scale windstorm connected with the cyclone Fabienne was untypical in its time of occurrence, and velocity of storm moving activity highly exceeded standard values for the season. The temperature drop on frontal border of 10 °C is also rather large. The major damages were caused by the storms on frontal border mainly on the territory of Germany, where the wind gusts reached extreme values 45 m.s^{-1} (162 km.h^{-1}). In the Czech Republic, the strongest wind gusts of about 35 m.s^{-1} (126 km.h^{-1}) were recorded mountains. Significant strong wind was observed in lowlands as well. For instance, in the meteo-station Karlov, located in Prague, wind gust reached values 27 m.s^{-1} (97 km.h^{-1}).

We have detected significant change in the dynamical pattern in stratosphere followed immediately after storm both in wind and temperature. General circulation pattern above Europe at 0.1 hPa before the storm Fabienne event can be classified/characterized as part of the stratosphere in normal condition in September. Based on that, we attribute the overall change of the stratospheric circulation/dynamics to the strong wave-field that was launched upward from the fast moving mesoscale system.

At the time of Fabienne event, ionosphere was slightly influenced by minor to moderate geomagnetic storm that occurred one day before. According to the evolution of Kp index and ionospheric plasma parameters (TEC and foF2) ionosphere was already in the recovery phase of the geomagnetic storm. Nevertheless, the observed disturbances are induced both by geomagnetic storm and convective activity in the lower laying atmosphere.

We have found significant departures from typical values of ionospheric parameters shortly after transition of the cold front across the observation point. We have detected sudden strong increase of wave-like activity on the directograms and CDS records. Detected strong echo on directograms shows strong and rapid changes in the horizontal plasma motion. During the observation, there was no prevailing plasma motion direction. It rather accounts for turbulent flow within F-layer. In the strong echo in directograms attributed to the storm, there is no characteristic prevailing motion, but sudden changes in direction are observed through the event. Time-limited increase of plasma drift in North and East direction has been

Ann. Geophys. Discuss., https://doi.org/10.5194/angeo-2019-26
Manuscript under review for journal Ann. Geophys.
Discussion started: 5 March 2019

detected together with decrease of velocity of the vertical plasma flow. Wave-like oscillations are present within ionospheric plasma all the time. In the WPS spectra of critical frequency we have detected change of the spectral content during day of the Fabienne event compared to preceding day. We have noticed decrease of F layer thickness during day of the Fabienne event. Irregular stratification of the ionosphere is confirmed by spread-echo recorded by Digisonde during afternoon and night on 23 September till morning 24 September. CDS data show significant change in spectral content, shape and power of the registered signal corresponding to modulation by waves propagating from convective system.

On the above summarized results we conclude that mesoscale systems are effective sources of atmospheric disturbances that can reach ionospheric heights and significantly alter atmospheric and ionospheric conditions. Convective system Fabienne affected Earth's atmosphere on a continental scale and up to F-layer heights. Even during periods of geomagnetic disturbance, minor to moderate geomagnetic storm, the contribution of the lower atmosphere to the ionospheric dynamics cannot be neglected. Our experimental result is in agreement with theoretical study of Pedatella (2018) that internal atmosphere variability should be taken into account even during geomagnetic disturbances.

Code availability

http://umlcar.uml.edu/digisonde.html

Data availability

Data used for the paper can be downloaded via followig sites:
https://www.ventusky.com/
https://www.wetterkontor.de/
http://wetter3.de,
http://www.ufa.cas.cz/institute-structure/department-of-meteorology/present-weather-sporilov.html
http://aeolus-ds.eo.esa.int/socat/L1B_L2_Products
https://disc.gsfc.nasa.gov/daac-bin/FTPSubset2.pl
http://giro.uml.edu/
http://digisonda.ufa.cas.cz/
http://www.ufa.cas.cz/files/OHA/M_Doppler_system.pdf
http://datacenter.ufa.cas.cz/
http://gnss.be/Atmospheric_Maps/ionospheric_maps.php
https://www.gfz-potsdam.de/en/kp-index/

Team list
Petra Koucká Knížová, Kateřina Podolská, Kateřina Potužníková, Daniel Kouba, Zbyšek Mošna, Josef Boška and Michal Kozubek

Author contribution
Petra Koucká Knížová (PKK) – DPS 4D ionogram data scaling, analyses and interpretation, first draft of the paper

Kateřina Podolská (KAPO) – AEOLUS data analyses and interpretation, CDS data analyses and interpretation.
Kateřina Potužníková (KACA) – meteorology data preparation and interpretation
Daniel Kouba (DK) – DPS 4D settings, Drift data analyses
Zbyšek Mošna (ZM) - TEC data analyses and interpretation, figure preparation
Josef Boška (JB) - DPS 4D data interpretation
Michal Kozubek (MK) – stratospheric data analyzes and interpretation

Competing interests.

Petra Koucká Knížová is one of the Special Issue Editors Annales Geophysicae.

Acknowledgements:

Authors would like to thank colleagues from the Institute of Atmospheric Physics CAS Marek Kašpar for synoptic interpretation of Fabienne cyclone peculiarities, and further Jaroslav Chum, Jiří Baše and František Hruška for maintenance of Doppler systems. Authors would like to acknowledge Global Ionosphere Radio Observatory (GIRO) and its mirror-site hosted in the Institute of Atmospheric Physics CAS.
Work of PKK, DK, ZM, JB was supported by the H2020 COMPET-2017 TechTIDE Project.
Work of KAPO was supported by project 18-01969S and work of MK by project 18-01625S of Czech Science Foundation.

References:

Alexander, M.J., Holton, J.R., and Durran, D.R.: The Gravity Wave Response above Deep Convection in a Small Line Simulation, Jour. of Atmos. Sci., 52, 12, 2212-2226, 1994.
Anthes, R. A.: Exploring Earth's atmosphere with radio occultation: contributions to weather, climate and space weather, Atmos. Measur. Tech., 4, 6, 1077-1103, DOI: 10.5194/amt-4-1077-2011, 2011.
Azeem, I., Yue, J., Hoffmann, L., Miller, S. D., Straka III, W. C. and Crowley G.: Multisensor profiling of a concentric gravity wave event propagating from the troposphere to the ionosphere, Geophys. Res. Lett., 42, 7874–7880, doi:10.1002/2015GL065903, 2015.
Boška**,** J. and Šauli, P.: Observations of gravity waves of meteorological origin in the F-region, Phys. and Chem. of the Earth Part C-Solar-Terrestial and Planetary Science. 26, 6, 425-428 ISSN 1464-1917, 2001.
Buonsanto, M. J.: Ionospheric storms – A review, Sp. Sci. Rev., 88, 3-4, 563-601, 1999.
Clilverd, M.A., Ulich, T., and Jarvis, M.J.: Residual solar cycle influence on trends in ionospheric F2-layer peak height, J. Geoph. Res. – Space Physics, 108, A12, 1450, 2003.
Chernigovskaya, M. A., Shpynev, B. G., and Ratovsky, K. G.: Meteorological effects of ionospheric disturbances from vertical radio sounding data, J. Atmos. Sol.-Terr. Phys., 136, 235-243, DOI: 10.1016/j.jastp.2015.07.006, 2015.
Chernigovskaya, M. A., Shpynev, B. G., Ratovsky, K. G., Belinskaya, A. Yu., Stepanov, A. E., Bychkov, V. V., Grigorieva, S. A., Panchenko, V. A., Korenkova, N. A., and Mielich, J.: Ionospheric response to winter stratosphere/lower mesosphere jet stream in the Northern Hemisphere as derived from vertical radio sounding data, J. Atmos. Sol.-Terr. Phys., 180, 126-136, DOI: 10.1016/j.jastp.2017.08.033, 2018.

Cnossen, I., and Franzke, Ch.: The role of the Sun in long-term change in the F-2 peak ionosphere: New insights from EEMD and numerical modeling, J. Geoph. Res.-Space Physics, 119, 10, 8610-8623, DOI: 10.1002/2014JA020048, 2014.

Chum, J., Liu, J.-Y., Podolska, K., and Sindelarova, T.: Infrasound in the ionosphere from earthquakes and typhoons, J. Atmos. Sol.-Terr. Phys., 171, Special Issue , 72-82, ISSN 1364-6826, 2018

Durand Y., Meynart R., Morançais D., Fabre F., and Schillinger M.: Results of the pre-development of ALADIN - the direct detection Doppler wind lidar for ADM/AEOLUS mission, poster at the Int. Laser Radar Conf., Matera, p. 247., ESA, European Space Agency, ALADIN, Doppler lidar working group report, SP-1112, 45 p., 1989.

Davies, K.: Ionospheric Radio, IEE Electromagnetic Waves Series 31, Peter Peregrinus LtD., ISBN 0 86341 168 X, 1990.

Fenrich, F.R. and Luhmann, J.G.: Geomagnetic response to magnetic clouds of different polarity, Geophys. Res. Lett., 25, Issue: 15, Pages: 2999-3002, DOI: 10.1029/98GL51180 , 1998.

Forbes, J.M., Palo, S.E., and Zhang, X.L.: Variability of the ionosphere, Jour. of Atmosph. and Sol.-Terr. Phys., 62, 8, 685-693, DOI: 10.1016/S1364-6826(00)00029-8, 2000.

Fritts, D.C., and Nastrom, G.D.: Sources of Mesoscale Variability of Gravity Waves. 2. Frontal, Convective, and Jet-stream Excitation, Jour. of Atmos. Sci., 49, 2, 111-127, DOI: 10.1175/1520-0469, 1992.

Garcia, R.R., and Solomon, S.: The Effect of Breaking Gravity-Waves on the Dynamics and Chemical-Composition of the Mesosphere and Lower Thermosphere, J. Geoph. Res. – Atmosph., 90, ND2, 3850-3868, DOI: 10.1029/JD090iD02p03850, 1985.

Gelaro, R. Gelaro,R., McCarty, W., Suáreza, M.J., Todlinga, R., Moloda, A., Takacsa, L., Randlesa, C.A., Darmenova, A., Bosilovicha,M.G., Reichlea, R., Wargana, K., Coya, L., Cullathera, R., Drapera, C., Akellaa, S., Bucharda, V., Conatya, A., da Silvaa, A.M., Gua, W., Gi-Kong Kima, Kostera, R., Lucchesia, R., Merkova, D., Nielsena, J.E., Partyka, G., Pawsona, S., Putmana, W., Rieneckera, M., Schuberta, S.D., Sienkiewicza, M., and Zhaoa, B.:The Modern-Era Retrospective Analysis for Research and Applications, Version 2 (MERRA-2). J. Climate, 30, 5419–5454, https://doi.org/10.1175/JCLI-D-16-0758.1, 2017.

Georgieva, K., Kirov, B., and Gavruseva, E.: Geoeffectiveness of different solar drivers, and long-term variations of the correlation between sunspot and geomagnetic aktivity, Phys. and Chem. of the Earth., 31, 1-3, 81-87, DOI: 10.1016/j.pce.2005.03.003, 2006.

Georgieva, K. Kirov, B., Koucká Knížová, P., Mošna, Z., Kouba, D., and Asenovska, Y.: Solar influences on atmospheric circulation, J. Atmos. Sol.-Terr. Phys., 90-91, SI, 15-25, ISSN 1364-6826, 2012.

Gompf, B., and Pecha, R.: Mie scattering from a sonoluminescing bubble with high spatial and temporal resolution, Phys. Rev. E 61(5), 5253–5256, 2000.

Goncharenko, L. P., Chau, J. L., Liu, H. -L., and Coster, A. J.: Unexpected connections between the stratosphere and ionosphere, Geophys. Res. Lett., 37, L10101, DOI: 10.1029/2010GL043125, 2010.

Gonzales, W. D., Joselyn, J. A., Kamied, Y., Kroehl, H.W., Rostoker, G., Tsurutani, B.T., and Vasyliunas, V.M.: What is Geomagnetic Storm, J. Geoph. Res. – Space Physics , 99, A4, 5771-5792, DOI: 10.1029/93JA02867, 1994.

Haldoupis, Ch.: Midlatitude Sporadic E. A Typical Paradigm of Atmosphere-Ionosphere Coupling, Space Sci. Rev., 168, 1-4, 441-46, DOI: 10.1007/s11214-011-9786-8, 2012.

Hargreaves, J.K.: The solar-terrestrial environment, Cambridge Atmospheric and Space Science Series, Cambridge University Press, ISBN 0 521 42737 1, 1992.

Hines, C. O.: Internal Atmospheric Gravity Waves at Ionospheric Heights, Can. Jour. of Phys., 38, 11, 1441-1481, https://doi.org/10.1139/p60-150, 1960.
Hines, C. O.: The upper atmosphere in motion, Quart. J. Roy. Meteorol. Soc., 89, 1, 1963.
Hines, C. 0., Dynamical heating of the upper atmosphere, J. Geophys. Res., 70, 177, 1965.
Hines, C. 0., Some consequenceosf gravity-wave critical layers in the upper atmosphere, J. Atmosph. Terrest. Phys., 30, 837, 1968.
Holton, J.R.: The influence of gravity wave breaking on the general circulation of the middle atmosphere, Jour. of Atmosph. Sci., 40,2497-2507, DOI, 1983.
Hooke, W.: Quasi-Stagnation Levels in the Ion Motion Induced by Internal, Atmospheric Gravity Waves at Ionospheric Heights, J. Geoph. Res., 248-249, 76, 1, 1971.
Hooke, W.: The Ionospheric Response to Internal Gravity Waves, 1. The F2 Region Response, J. Geoph. Res. - Space Phys., 75, 28, pp, 1970.
Hooke, W.: Ionospheric Response to Internal Gravity Waves, 3. Changes in the Densities of the Different Ion Species, J. Geoph. Res. - Space Phys., 75, 34, pp, 1970.
Jones S. C., Harr P. A., Abraham J., Bosart L. F., Bowyer P. J., Evans J. L., Hanley D. E., Hanstrum B. N., Hart R. E., Lalaurette F., Sinclair M. R., and Smith R. K., and Thorncroft Ch.,: The Extratropical Transition of Tropical Cyclones: Forecast Challenges, Current Understanding, and Future Directions. Weather and Forecasting 18:6,1052-1092. 1-Dec-2003.
Kakad, B., Kakad, A., Ramesh, D. S., and Lakhina, G. S.: Diminishing activity of recent solar cycles (22-24) and their impact on geospace, Jour. of Space Weather and Space Clim., 9, A01, DOI: 10.1051/swsc/2018048, 2019.
Kašpar, M., Müller, M., Crhová, L., Holtanová, E., Polášek, J.F., Pop, L., and Valeriánová, A.: Relationship between Czech windstorms and air temperature, Int. J. Climatol., 37, 11–24, doi: 10.1002/joc.4682, 2017.
Kašpar, M.: Objective frontal analysis techniques applied to the extreme/non-extreme precipitation events, Studia geoph. et geod., 47, 605–631. doi: 10.1023/A:1024771820322, 2003.
Kopáček J., and Bednář J.: Jak vzniká počasí [How the weather works] Karolinum, 228 pp., ISBN 8024610027, 2009. in Czech
Kouba, D., Boška, J., Galkin, I. A., Santolík, O., and Šauli, P.: Ionospheric drift measurements: Skymap points selection. Radio Sci.. 43, 1, RS1S90/1-RS1S90/11 ISSN 0048-6604, 2008.
Kouba, D. and Chum, J.: Ground-based measurements of ionospheric dynamics, Jour. of Space Weather and Space Clim., 8, 2018.
Kouba, D. and Koucká Knížová, P.: Ionospheric vertical drift response at a mid-latitude station. Adv. Space Res., 58, 1, 108-116, 2016.
Kouba, D., and Koucká Knížová, P.: Analysis of digisonde drift measurements quality, J. Atmos. Sol.-Terr. Phys., 90-91, 212-221, 2012.
Koucká Knížová, P., Mošna, Z., Kouba, D., Potužníková, K., and Boška, J.: Influence of meteorological systems on the ionosphere over Europe, Jour. of Atmosph. and Sol.-Terr. Phys., 136 B, 244-250, 2015.
Koucká Knížová, P., Georgieva, K., Mošna, Z., Kozubek, M., Kouba, D., Kirov, B., Potužníková, K., and Boška, J.: Solar signals detected within neutral atmospheric and ionospheric parameters, J. Atmos. Sol.-Terr. Phys., 171, 147-156, DOI: 10.1016/j.jastp.2017.12.003, 2018
McDonald, S. E., Sassi, F., Tate, J., McCormack, J., Kuhl, D. D., Drob, D. P., Metzler, C., and Mannucci, A. J.: Impact of non-migrating tides on the low latitude ionosphere during a

sudden stratospheric warming event in January 2010, J. Atmos. Sol.-Terr. Phys., 171, 188-200, DOI: 10.1016/j.jastp.2017.09.012, 2018.

Lastovička, J.: Forcing of the ionosphere by waves from below, J. Atmos. Sol.-Terr. Phys., 68, 3-5, 479-497, 2006.

Laštovička, J., Solomon, S., and Qian, L.: Trends in the Neutral and Ionized Upper Atmosphere, Space Sci. Rev., 168, 1-4, 113-145, DOI: 10.1007/s11214-011-9799-3, 2012.

Laštovička, J.: On the role of ozone in long-term trends in the upper atmosphere-ionosphere system, Ann. Geophys., 30, 5, 811-816, DOI: 10.5194/angeo-30-811-r012, 2012.

Leamon, R. J., Canfield, R. C., and Pevtsov, A. A.: Properties of magnetic clouds and geomagnetic storms associated with eruption of coronal sigmoids. J. Geoph. Res.-Space Phys. , 107, A9 , 1234, DOI: 10.1029/2001JA000313, 2002.

Liu, C. L., Kirchengast, G., Syndergaard, S., Kursinski, E. R., Sun, Y. Q., Bai, W. H., and Du, Q. F.: A review of low Earth orbit occultation using microwave and infrared-laser signals for monitoring the atmosphere and climate, Adv. Space Res., 60, 12, 2776-2811, DOI: 10.1016/j.asr.2017.05.011, 2017.

Mathews, J. D.: Sporadic E: current views and recent progress. J. Atmos. Sol.-Terr. Phys., 60 (4), 413–435, 1998.

Pedatella, N.M., and Liu H.-L.: The Influence of Internal Atmospheric Variability on the Ionosphere Response to a Geomagnetic Storm, Geoph. Res. Lett., 45, 10, 4578-4585, 2018.

Perrone, L., Mikhailov, A., Cesaroni, C., Alfonsi, L., De Santis, A., Pezzopane, and M., Scotto, C.: Long-term variations of the upper atmosphere parameters on Rome ionosonde observations and their interpretation, Jour. of Space Weather and Space Clim., 7, A21, DOI: 10.1051/swsc/2017021, 2017.

Prölss, G. W.: Physics of the Earth ´s Space Environment. An Introduction. Springer, 2004. ISBN 3-540-21426-7, 2004.

Reinisch, B.W.: Modern Ionosondes, in Modern Ionospheric Science, edited by Kohl, H., Rüster, R., and Schlegel, K., EGS, 37191 Katlenburg-Lindau, Germany, 440-458, 1996.

Reinisch, B.W., Huang, X., Galkin, I.A., Paznukhov, V., and Kozlov, A.: Recent advances in real-time analysis of ionograms and ionospheric drift measure- ments with digisondes. J. Atmos. Sol.-Terr. Phys., 67, 1054–1062, 2005

Rishbeth, H.: How the thermospheric circulation affects the ionospheric F2-layer, J. Atmos. Sol.-Terr. Phys., 60, 14, 1385-1402, 1998.

Roininen, L., Laine, M., and Ulich, T.: Time-varying ionosonde trend: Case study of Sodankyla h(m)F(2) data 1957-2014, J. Geoph. Res. - Space Phys., 120, 8, 6851-6859, DOI: 10.1002/2015JA021176, 2015.

Roux, S.G., Koucka Knizova, P., Mosna, Z., and Abry., P. Ionosphere fluctuations and global indices: A scale dependent wavelet-based cross-correlation analysis, J. Atmos. Sol.-Terr. Phys., 90–91, 186–197, 2002.

Sanders, F., 1986a: Explosive cyclogenesis over the west-central North Atlantic Ocean, 1981–1984. Part I: Composite structure and mean behavior. Mon. Wea. Rev., 114, 1781–1794.

Sauli, P. and Boska, J.:Tropospheric events and possible related gravity wave activity effects on the ionosphere, J. Atmos. Sol.-Terr. Phys., 63, , 945-950 ISSN 0021-9169, 2001.

Solomon, S.C. and Qian, L.Y.: Solar extreme-ultraviolet irradiance for general circulation models, J. Geoph. Res.-Space Phys. , 110, A10, A10306, DOI: 10.1029/2005JA011160, 2005.

Tan D. G. H. and Andersson E.: Simulation of the yield and accuracy of wind profile measurements from the Atmospheric Dynamics Mission (ADM-Aeolus). Reading, UK, European Centre for Medium-range Weather Forecast (ECMWF), Research Department, Tech. Memo. 431, 29 p, 2004.

Vadas S. and Fritts, D.C.: Thermospheric responses to gravity waves: Influences of increasing viscosity and thermal diffusivity, J. Geoph. Res.-Atmosph., 110, D15, D15103, DOI: 10.1029/2004JD005574, 2005.

Vadas, S.: Horizontal and vertical propagation and dissipation of gravity waves in the thermosphere from lower atmospheric and thermospheric sources, J. Geoph. Res. -Space Physics, 112, A6, A06305, 2007.

Vadas, S. and Liu, H-L.: Generation of large-scale gravity waves and neutral winds in the thermosphere from the dissipation of convectively generated gravity waves, J. Geoph. Res. -Space Phys., 114, A10310, 2009.

Vadas, S. and Nicolls, M.J.: The phases and amplitudes of gravity waves propagating and dissipating in the thermosphere: Theory, J. Geoph. Res. – Space Phys., 117, A05322, doi:10.1029/2011JA017426, 2012

Vadas, S.L., Zhao, J., Chu, X., and Becker, E.: The Excitation of Secondary Gravity Waves From Local Body Forces: Theory and Observation, J. Geoph. Res.- Atmosph., 123, 9296-9325, https://doi.org/10.1029/2017JD027970, 2018.

Whitehead, J.D.: The formation of the sporadic E layer in terperate zones, J. Atmos. Sol.-Terr. Phys., 20, 49–58, 1961.

Whitehead J.D.: Sporadic E layers; history and recent observations, Adv. Space Res., Volume 10, Issue 10., Pages 85-91, https://doi.org/10.1016/0273-1177(90)90013-P, 1990.

Yigit, E., Koucká Knížová, P., Georgieva, K., and Ward, W.: A review of vertical coupling in the Atmosphere-Ionosphere system: Effects of waves, sudden stratospheric warmings, space weather, and of solar activity, J. Atmos. Sol.-Terr. Phys., 141, 1-12, 2016.

Web pages

https://earth.esa.int/web/guest/missions/esa-operational-eo-missions/aeolus

http://www.met.wur.nl/education/atmospract/unit9/thetaw%20and%20fronts.pdf

https://www.eswd.eu

http://www.ufa.cas.cz/files/OHA/M_Doppler_system.pdf\

http://ulcar.uml.edu/directograms.html

Ann. Geophys. Discuss., https://doi.org/10.5194/angeo-2019-26
Manuscript under review for journal Ann. Geophys.
Discussion started: 5 March 2019

Annales Geophysicae Discussions
Open Access

\

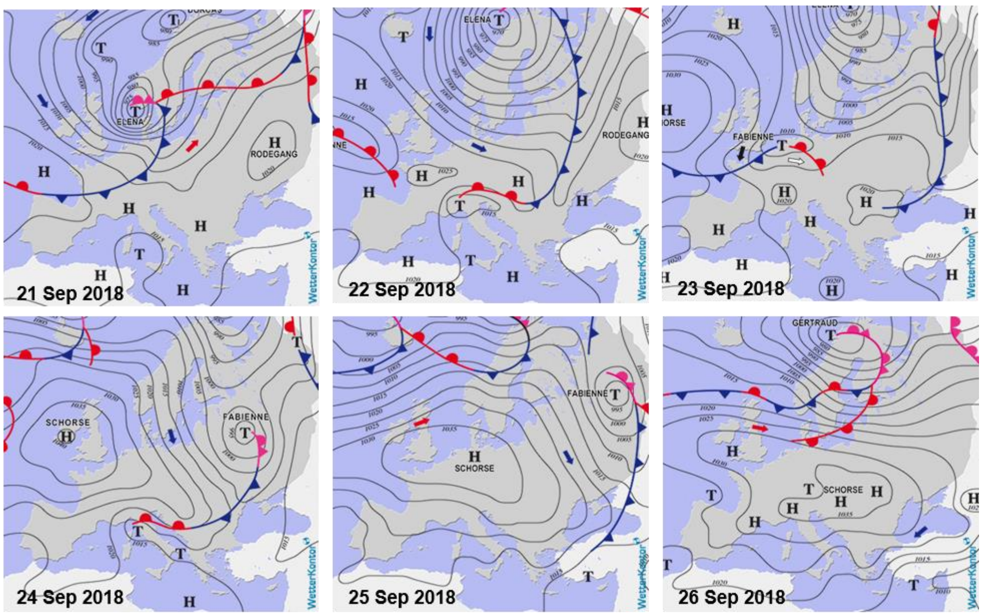

Fig. 1. Surface pressure maps provided by Wetterkontor, from www.wetterkontor.de. Surface pressure is plotted with solid lines with 5 hPa step. Atmospheric fronts (red curved lines with red semi-circles that point in the direction of warm front, blue curved line with blue triangles that point in the direction of cold front and purple line with alternating triangles and semi-circles pointing in the direction in the occluded front is moving), the location of the centres of high (H) and low (T) pressure systems are also presented.

Ann. Geophys. Discuss., https://doi.org/10.5194/angeo-2019-26
Manuscript under review for journal Ann. Geophys.
Discussion started: 5 March 2019

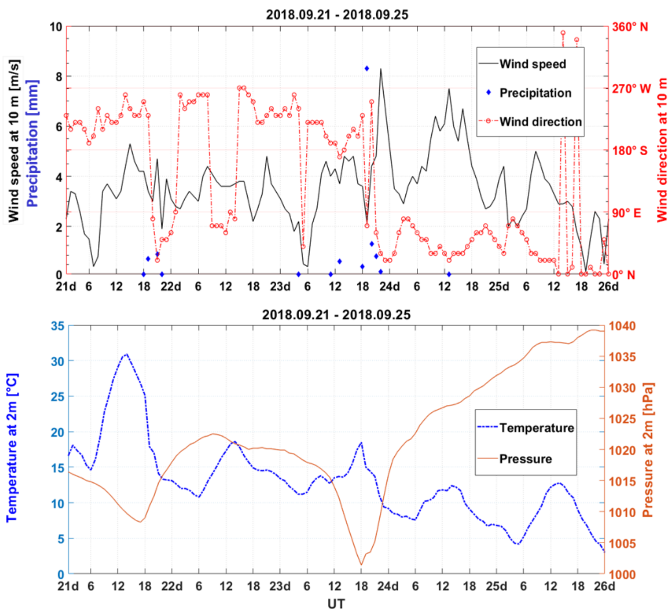

Fig.2. Hourly averages surface observations at IAP meteorological station. Atmospheric pressure, air temperature and precipitation amount are measured at the two meters height above the surface, wind speed and direction at ten meters height above the surface.

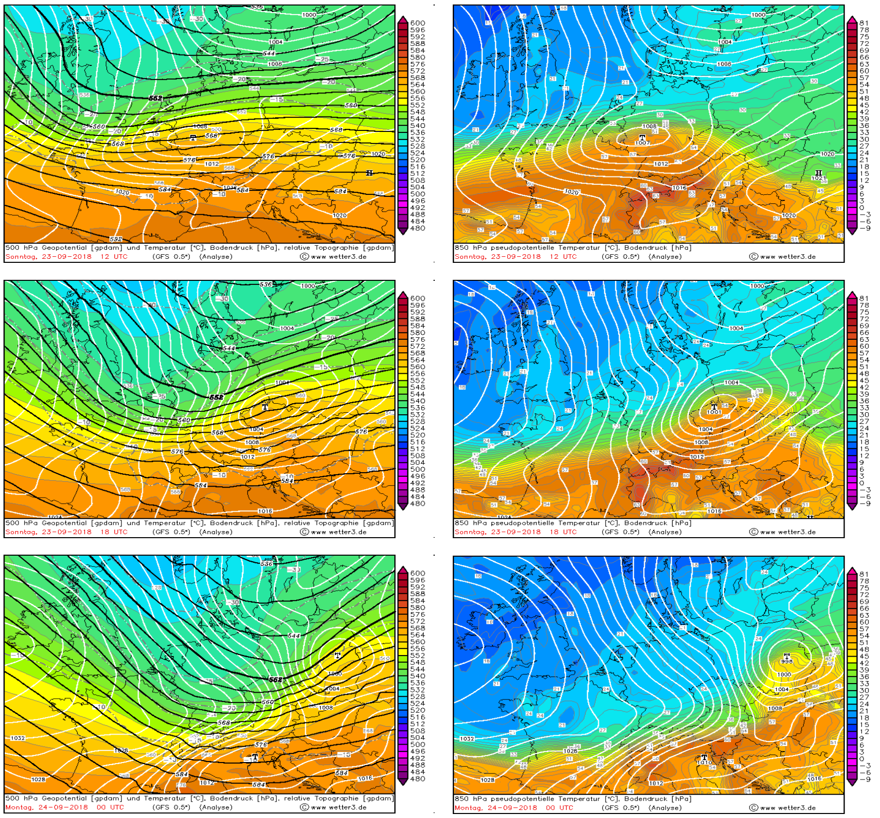

Fig.3. Distribution of the geopotential field (black lines) and temperature (gray dashed lines) at level of 500 hPa, of the surface pressure field (white lines), and of relative topography 500–1000 hPa (color field). The 500 hPa is given in units of 10 geopotential decameter (gpdam), the temperature in °C, the surface pressure in hPa, and the 500/1000 hPa thickness in gpdam. Isohypses and thickness are 4 gpdam apart, isobars 2 hPa and isotherms 5 °C. The thickness or difference in heights between the 1000 hPa (surface) and 500 hPa levels varies on temperature and moisture (is a function of average virtual temperature), thus the color field regions depicted the average temperature of the troposphere. (Orange/red values indicate warm tropical air, blue/indigo indicate artic air.) **Right panels**: Analysis of pseudo-potential temperature in 850 hPa pressure level in °C (color field and isotherms - gray lines, 3 °C apart) and surface pressure field (isobars - white lines, 2 hPa apart). The pseudo-potential temperature is conservative in association with the moisture thus it allows to compare temperature of air masses in lower troposphere regardless of their humidity.

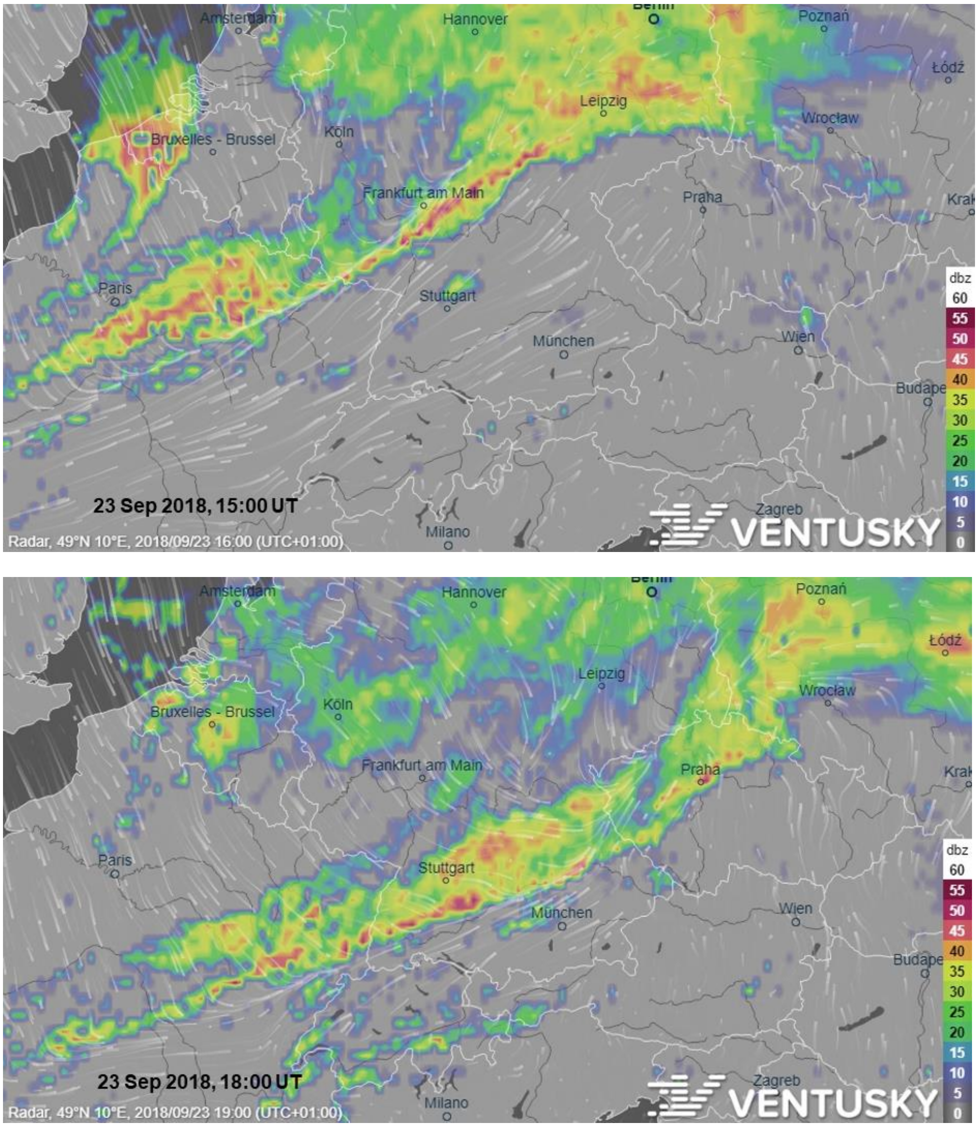

Fig. 4. Horizontal maximum projection of radar reflectivity from the European radar provided by VentuSky (https://www.ventusky.com). There is a rapid shift of the strong thunderstorms line (squall line) by 350 km per three hours. White lines illustrate the wind speed at ten meters above the ground. The colour scale indicates the radar reflectivity in 5 dBZ increments. The scale demonstrates exponential dependence of precipitation intensity [mm h^{-1}] on radar reflektivity [dBZ]. The value of 55 dBZ (dark purple) corresponds to the instantaneous value of intensity of convective precipitation 100 mm h^{-1}.

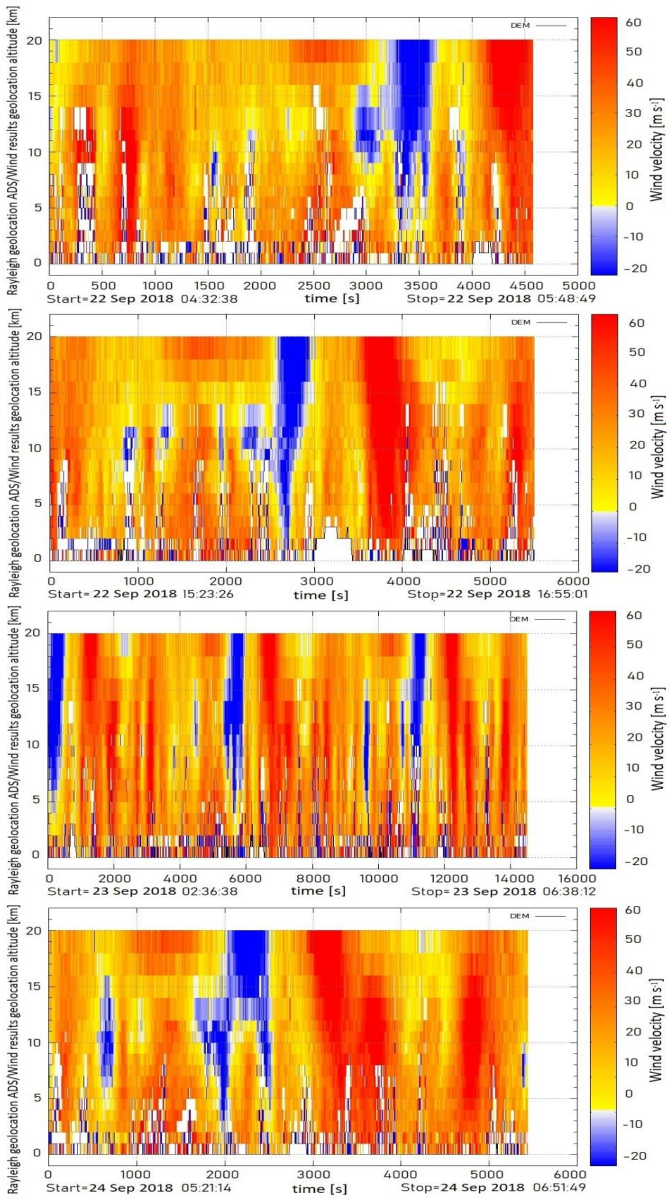

Fig.5. Aeolus Rayleigh scattering observations of wind profiles up to 20 km. The MDS wind profiles (positive towards the instrument) measured during the orbit numbers 513 and 514 on 22–24 September 2018 between 04:32 and 06:51 UTC using the MDS Rayleigh scattering. The blue areas indicate periods during which the wind speed variations introduced by the Rayleigh response fluctuations are negative.

Ann. Geophys. Discuss., https://doi.org/10.5194/angeo-2019-26
Manuscript under review for journal Ann. Geophys.
Discussion started: 5 March 2019

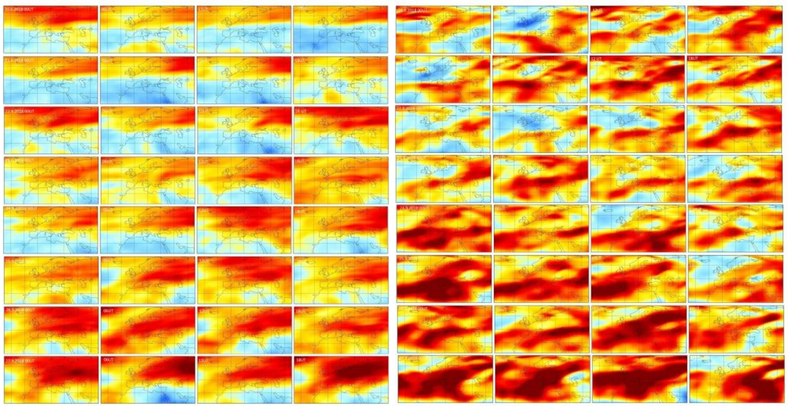

(a) (b)

Fig. 6. Stratospheric wind above Europe at 1hPa (panel a), and at 0.1hPa (panel b). Red color represent eastward wind, blue represents westward wind.

Ann. Geophys. Discuss., https://doi.org/10.5194/angeo-2019-26
Manuscript under review for journal Ann. Geophys.
Discussion started: 5 March 2019

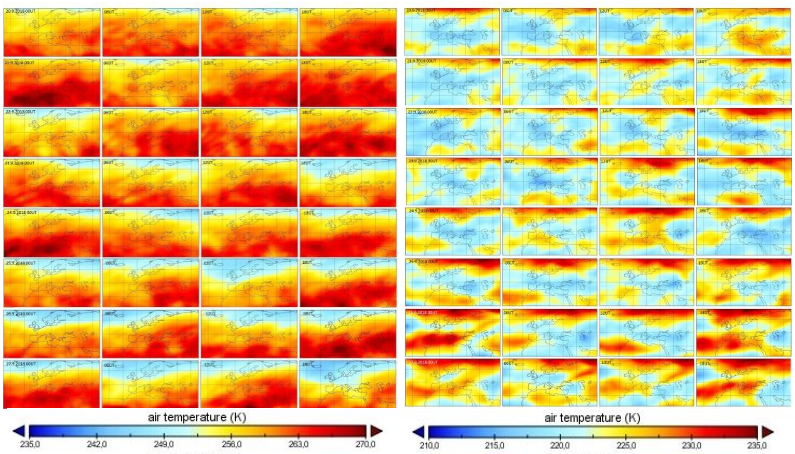

(a) **(b)**

Fig. 7. Stratospheric temperature above Europe at 1hPa (panel a; temperature in the range 235 – 270 K) and at 0.1 hPa (panel b; temperature in the range 210 – 235 K).

Ann. Geophys. Discuss., https://doi.org/10.5194/angeo-2019-26
Manuscript under review for journal Ann. Geophys.
Discussion started: 5 March 2019

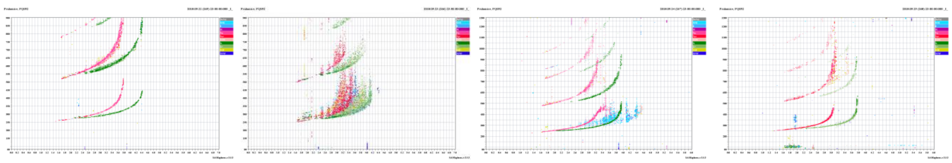

Fig. 8. Sequence of ionograms recorded during local night at around 23 UT presented in a standard DPS 4D output format .

Ann. Geophys. Discuss., https://doi.org/10.5194/angeo-2019-26
Manuscript under review for journal Ann. Geophys.
Discussion started: 5 March 2019

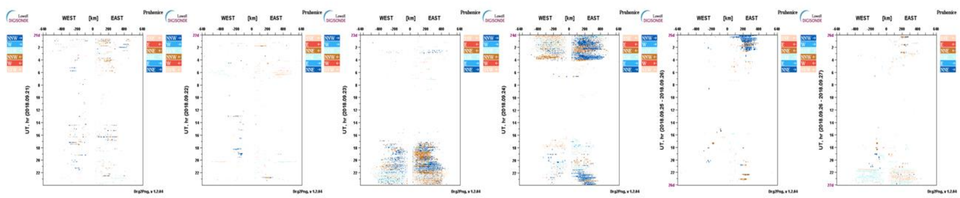

Fig. 9. Sequence of directograms recorded on 21–26 September presented in a standard DPS 4D output format.

Ann. Geophys. Discuss., https://doi.org/10.5194/angeo-2019-26
Manuscript under review for journal Ann. Geophys.
Discussion started: 5 March 2019

Annales Geophysicae Discussions Open Access

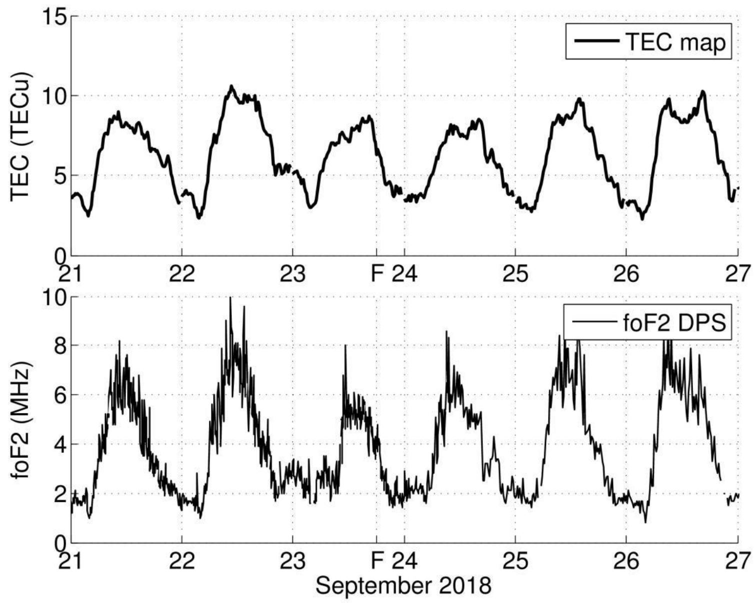

Fig. 10. Diurnal courses of Total Electron Content (upper panel) and critical frequency foF2 (bottom panel) above station Pruhonice "F" denotes time of passage of the storm Fabienne over the station.

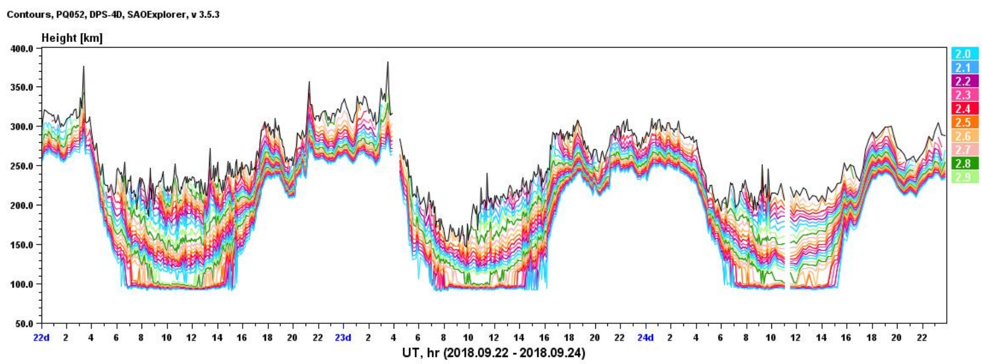

Fig.11. Variability of true-height reflection at fixed frequencies recorded during 22–24 September for frequency range 2–6 MHz with 0.1 MHz step, in a standard DPS 4D output format.

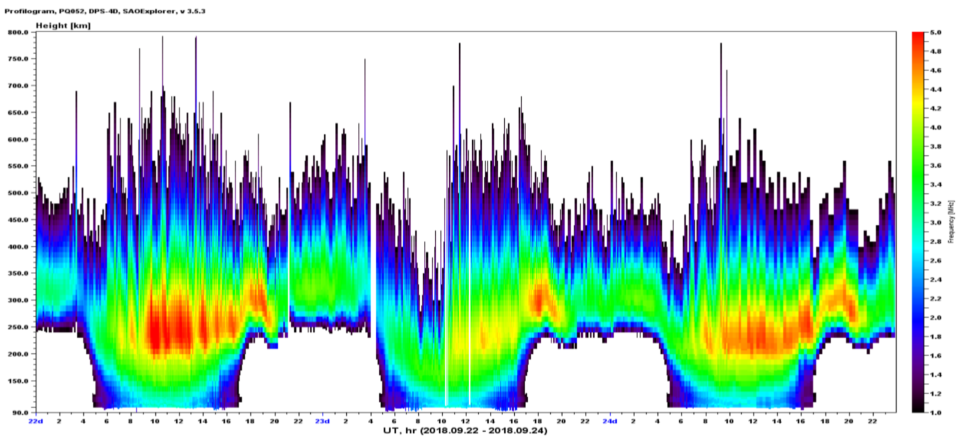

Fig. 12. Detail of profilograms in frequency – 22 September–24 September presented in a standard DPS 4D output format.

Ann. Geophys. Discuss., https://doi.org/10.5194/angeo-2019-26
Manuscript under review for journal Ann. Geophys.
Discussion started: 5 March 2019

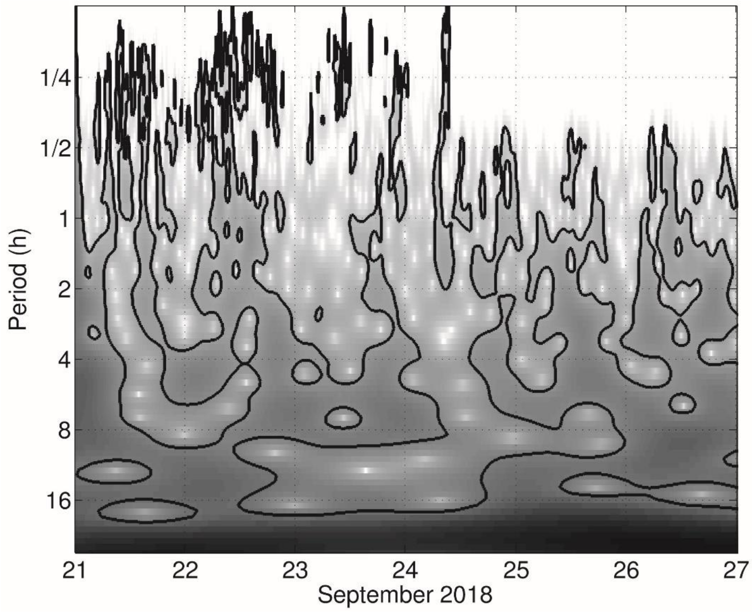

Fig.13. Wavelet Power Spectra of critical frequency foF2 for 21–27 September, 2018.

Ann. Geophys. Discuss., https://doi.org/10.5194/angeo-2019-26
Manuscript under review for journal Ann. Geophys.
Discussion started: 5 March 2019

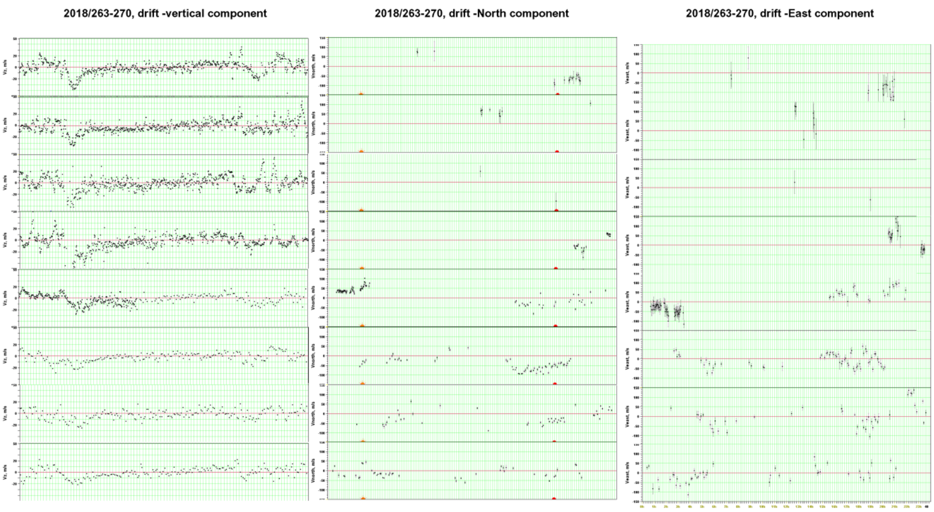

(a) (b) (c)

Fig. 14. Components of ionospheric plasma drift obtained by Digisonde DPS 4D – (a) vertical component; (b) North component; (c) East component presented in a standard DPS 4D output format.

Ann. Geophys. Discuss., https://doi.org/10.5194/angeo-2019-26
Manuscript under review for journal Ann. Geophys.
Discussion started: 5 March 2019

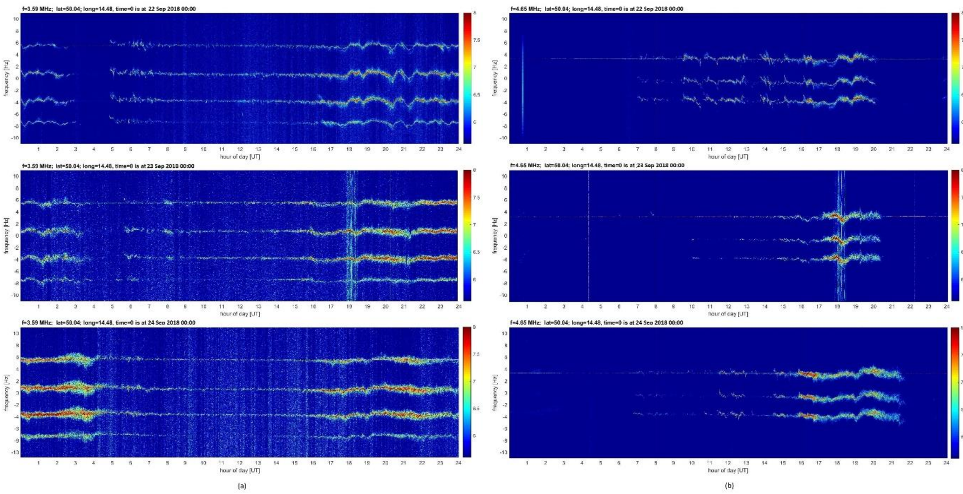

(a) (b)

Fig. 15. Continuous Doppler Sounding measurement on three consequent days 22–24 September on frequency 3.59 MHz (a) and 4.65 MHz (b).